Influence of Electrode Placement on the Morphology of In Silico 12 Lead Electrocardiograms

Karli Gillette[1,2], Matthias AF Gsell[1], Anton J Prassl[1], Gernot Plank[1,2]

[1] Gottfried Schatz Research Center : Biophysics, Medical University of Graz, Graz, Austria
[2] BioTechMed-Graz, Graz, Austria

Abstract

Introduction: *Multiple clinical studies have aimed to assess the influence of electrode placement on 12 lead electrocardiogram (ECG) morphology. However, a study has not yet been conducted in silico. We therefore aim to systemically investigate the influence of electrode positioning on the morphology of the 12 lead ECG using a cardiac model of electrophysiology under both healthy sinus rhythm and right bundle branch block (RBBB).*

Methods: *A biophysically-detailed model of ventricular electrophysiology of a single subject was used to model body surface potential maps during healthy sinus rhythm and RBBB. A systematic automatic perturbation of all electrodes from the original subject configuration was performed to replicate clinical variation. For each variation in electrode placement, the 12 lead ECG was computed under both conditions. Quantitative differences were assessed using a time-averaged normalized L_2 norm.*

Results: *The precordial leads that lie in closer proximity to the heart, primarily V2 and V3, experienced the largest morphological changes from vertical electrode movement. Morphological variation in the augmented Goldberger and Einthoven leads resulted predominantly from LA electrode placement. The possibility of a false diagnosis of RBBB during sinus rhythm due to improper electrode placement was also demonstrated.*

1. Introduction

The 12 lead electrocardiogram (ECG) is considered the gold standard for initial diagnosis and long-term monitoring of a variety of common cardiovascular diseases including heart attacks and ventricular arrhythmic disorders. Large variation in electrode positioning has been observed, however, even among trained practitioners regardless of standardized guidelines [1]. Such deviations induce morphological changes in the recorded 12 lead ECG potentially leading to improper patient diagnosis and treatment [2]. More recently, such morphological changes have also been an important research topic for computer-based diagnostic approaches or the generation of cardiac digital twins.

Recent clinical studies have therefore aimed to understand the influence of electrode placement on the morphology of the 12 lead ECG by manually varying electrode positions or selecting subsets of electrodes from body surface potential maps (BSPMs) [2]. However, such studies are typically performed on a small patient population within a particular pathological subgroup, tend to have low or inconsistent spatial resolution of electrode positioning due to manual placement, or require artificial signal interpolation from BSPM recordings. Furthermore, information on the actual underlying electrical activity of the heart is of limited accuracy or afflicted with significant uncertainty. Biophysical cardiac models of electrophysiology (EP) capable of modeling a variety of cardiovascular diseases therefore provide a natural means to conduct such simulation studies. However, a systematic *in silico* study using a cardiac model of EP has not yet been conducted.

We thus aimed to conduct an *in silico* study to systematically assess the morphological variation of the 12 lead ECG and resulting potential for false diagnosis due to electrode displacement. Healthy sinus rhythm and right bundle branch block (RBBB) for a single subject was modeled using a biophysically-detailed *in silico* model of ventricular EP previously personalized to the measured 12 lead ECG under sinus rhythm recorded using exactly known image-based electrode positions. Systematic perturbations of the known electrode positioning were then performed automatically using universal torso coordinates (UTCs) under both conditions. Resultant morphological variation in the 12 lead ECG was quantified using a time-averaged normalized L_2 norm.

2. Methods

2.1. Model Construction

An anatomically-specific model of a single subject (male, 45 years of age) was taken from a model cohort

 ISSN: 2325-887X DOI: 10.22489/CinC.2021.007

of 12 healthy subjects previously generated from clinical magnetic resonance imaging data [3]. A 12 lead ECG had been measured on the healthy subject using electrodes compatible with magnetic resonance imaging left intact during initial cardiac imaging. Primary tissues of lungs, atria, blood pools, ventricles, and general torso tissue were accounted for. The model had been meshed to an average resolution of $1206\,\mu\mathrm{m}$; $4171\,\mu\mathrm{m}$ on the torso surface and $998\,\mu\mathrm{m}$ within the heart deemed suitable for simulation (Sec. 2.2). To facilitate the automated prescription and manipulation of all EP parameters for simulation, including electrode placement, the model had been retrofitted with an abstract reference frame consisting of both a modified implementation of universal ventricular coordinates (UVCs) and UTCs [3].

2.2. Cardiac Simulation

The model was first constructed to generate a sinus rhythm matching the measured 12 lead ECG of the single subject to ensure the biophysical fidelity of the model. The ventricular conduction system was represented using an improved version of the biophysically-detailed and steerable representation of the His-Purkinje system (HPS) controlled using UVCs detailed in [4]. During sinus, the HPS was assumed to comprise 5 fascicles rooted in the endocardium: 3 within the left ventricle, one in the right-ventricular septum, and one corresponding to the right-ventricular moderator band. An artificial His-bundle system was automatically constructed to connect the fascicles. Under RBBB, an electrical block was facilitated in a proximal right-ventricular branch site prohibiting subsequent activation within the right-ventricular branch of the network. The complete network comprised approximately $96\,\mathrm{k}$ nodes and $110\,\mathrm{k}$ branches due to a $500\,\mu\mathrm{m}$ spatial discretization. A total of $8.70\,\mathrm{k}$ Purkinje-myocardial junctions were assigned. A rapid conduction velocity of $2.00\,\mathrm{m\,s^{-1}}$ was assigned along the Purkinje fibers. Anterograde and retrograde delays between HPS and ventricular myocardium of $14.00\,\mathrm{ms}$ and $4\,\mathrm{ms}$, respectively, were assigned [5].

Remaining ventricular EP parameters during sinus rhythm for the simulations were prescribed according to experimental, clinical, and physiological studies. General myocardial conduction velocities were assigned $0.70\,\mathrm{m\,s^{-1}}$ [6] along the longitudinal myocardial fiber orientations with an off-axis ratio of 0.42 [7]. Fiber orientations within the myocardium were implemented using a rule-based algorithm [8] and ranged from $-60°$ on the endocardium to $60°$ on the epicardium. Heterogeneous conductivities within the ventricles were assigned according to [7]. Tissues within the torso, lungs, atria and blood pools were assigned isotropic conductivities according to the nominal values reported in [9]. The cellular action potential was represented using the simplified Mitchel-Schaeffer phenomenological model [10] using parameter settings according to [3]. Transmural, apicobasal, anterior-posterior, and ventricular gradients guiding heterogeneous ventricular repolarization for T-wave morphology were prescribed using a weighted technique based on UVCs [3].

Ventricular sources and the potentials within the torso volume were simulated using the reaction-Eikonal method run in pseudo-bidomain mode [11] to compute extracellular potential fields throughout the torso. Activation of the network in all conditions was initiated at the exit site of the atrio-ventricular node. Simulations were conducted for a single ventricular beat assumed to last $450\,\mathrm{ms}$. BSPMs were taken from the set of all potentials on the torso surface for each condition (Fig. 1A).

3. Alteration of Electrode Placement

Coordinate locations of the subject electrodes were localized to nodes on the torso surface of the mesh using *meshtool* [12] and provided the baseline configuration for the study. All electrode positions were then linearly varied from the baseline configuration by $\pm 20\%$ along the longitudinal and $\pm 10\%$ rotational UTCs. Precordial electrodes of V1 through V4 were shifted further upwards by an additional 10% longitudinally to replicate observed clinical patterns in electrode placement [1].

For each new configuration, the 12 lead ECG was computed under healthy sinus rhythm and RBBB conditions. An amplitude scaling factor of 0.23, computed between the measured and simulated 12 lead ECG under sinus, was applied across all simulated 12 lead ECGs [3]. To provide a quantitative description of morphological change in the 12 lead ECG resulting from a given electrode movement from the baseline configuration, the time-averaged L_2 norm was computed for each lead and averaged across all leads for a given simulation run. Each L_2 norm was normalized to the highest observed L_2 norm under the given corresponding cardiac condition of either healthy sinus or RBBB.

4. Results

A similar trend in morphological variation in the 12 lead ECG (Fig. 1C) is observed under both sinus and RBBB (Fig. 1B). Upward movement of the V2 and V3 electrodes resulted in highest overall L_2 norm. Higher placement of the V1 and V2 electrodes, however, led to more visible changes due to an increasingly apparent rSr' pattern and T-wave inversion in these leads under both conditions. Within the precordial leads of V3 and V4, an opposite trend was observed. The Einthoven and augmented Goldberger limb leads, as well as V6, appeared relatively robust against electrode movement. Nonetheless, movement of the LA electrode led to slight S-wave slurring and R am-

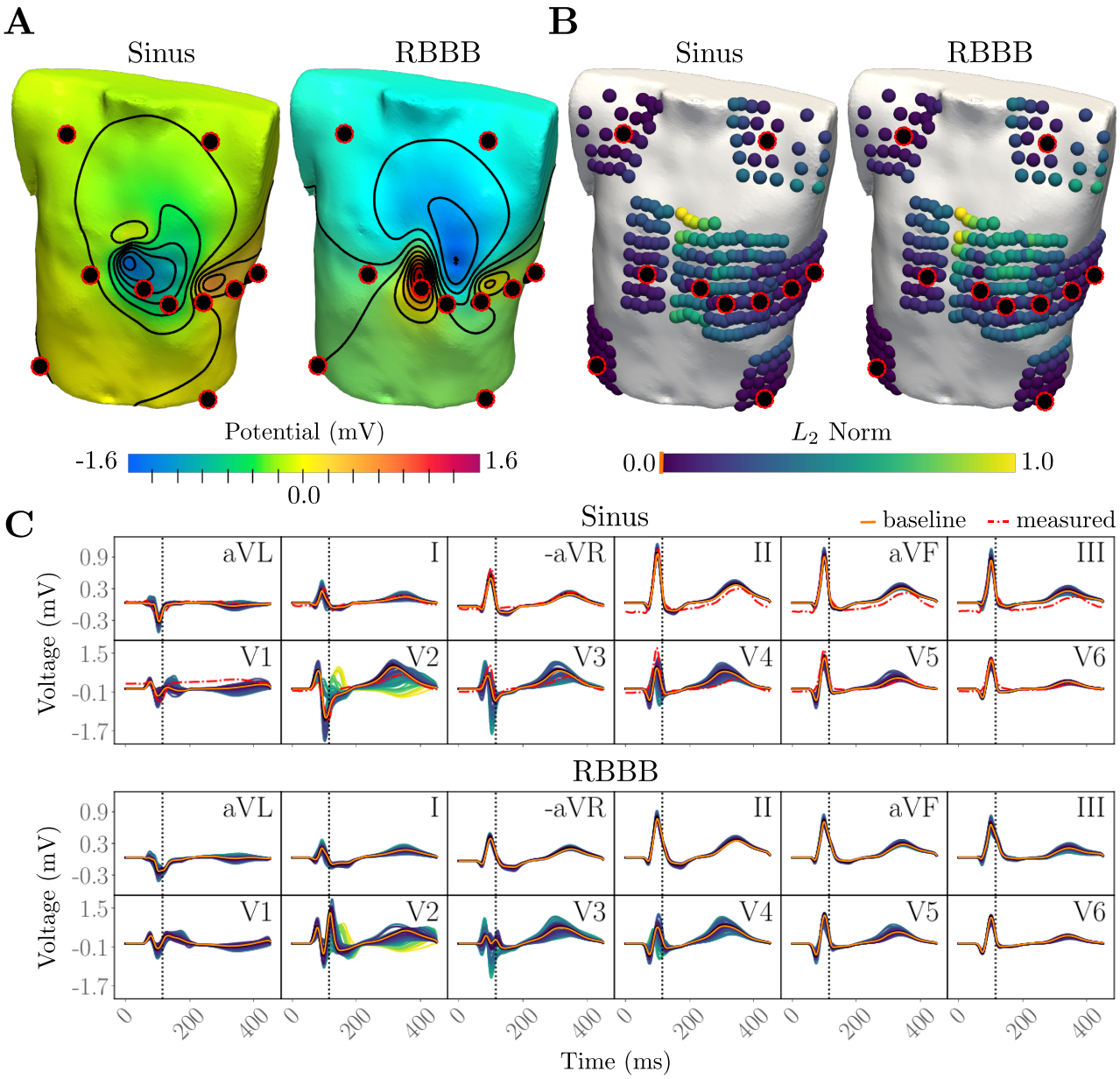

Figure 1. **A** Simulated BSPMs for a single subject during sinus-rhythm and RBBB shown at 115 ms following activation of the His-bundle system at the exit-site of the atrio-ventricular node. **B** Electrode variation on the torso surface from the clinically measured baseline configuration (red and black). **C** 12 lead ECGs under sinus (top) and RBBB (bottom). Coloration of the 12 lead ECG and electrode placements corresponds to normalized L_2 norm quantifying morphological variation. Baseline (orange) and measured (red) 12 lead ECGs are shown.

plitude elevation within -aVR and lead II, as well as any morphological variation observed in leads aVL and I.

5. Discussion

The influence that electrode placement has on the morphology of the 12 lead ECG, as well as on potential patient diagnosis, was investigated within a patient-specific model of ventricular EP within a single subject. In general, highest morphological variation was observed from upward electrode displacement of the precordial electrodes in close proximity to the projection of the cardiac dipole on the BSPM that resulted in a different projection viewpoint (Fig. 1). Alterations in the trigonometric proportions of the Einthoven triangle due to movement of the LA electrode also led to observed morphological changes in the

limb leads.

Initial findings suggest that a false diagnosis of RBBB could be feasible. The primary morphological characteristics of T-wave inversion and rSr' pattern observed in RBBB were also observed in leads V1 and V2 during healthy sinus rhythm given high, more centered placement of the V1 and V2 electrodes (Fig. 1). Other morphological features of RBBB, such as a slurred S-wave in V6 and prolonged QRS duration, were however not observed. High electrode placement of V1 and V2 should thus be accounted for during clinical diagnosis using the 12 lead ECG.

Systematic perturbations of electrode placements was conducted entirely automatically. Due to underlying mesh resolution, the variation in electrode placement was limited to approximately $4.20\,\mathrm{mm}$ resolution on the torso surface. Furthermore, a non-linear geometric sampling is observed due to the UTCs (Figure 1B). Linearization of the UTCs and increasing mesh resolution would overcome such restrictions.

Biophysical fidelity is an important consideration when utilizing cardiac models of EP for understanding mechanisms behind clinical diagnostics and treatments. Certain parameters that may influence the morphology of the ECG during electrode movement may have been neglected. For example, bones were not included within the model due to a lack of sufficient contrast within the clinical MRIs. Bones, however, may have electrical shielding effect particularly for the precordial leads. Within the single subject, however, a strong morphological agreement between the measured and simulated 12 lead ECGs (Fig. 1C) under sinus conditions was achieved for the single subject, suggesting that the primary aspects of ventricular EP needed for healthy sinus rhythm were considered. Comparison of simulation outcomes against both experimental and clinical data under all disease conditions across a larger model cohort of multiple subjects is also needed and would further elucidate the biophysical capabilities of the model.

.

Acknowledgments

This research was supported by the grant I2760-B30 from the Austrian Science Fund (FWF), by BioTechMed-Graz, Austria as a part of the BioTechMed-Graz Flagship Project ILearnHeart, and by the EU H2020 grant MedalCare 18HLT07.

References

[1] Rajaganeshan R, Ludlam C, Francis D, Parasramka S, Sutton R. Accuracy in ecg lead placement among technicians, nurses, general physicians and cardiologists. International journal of clinical practice 2008;62(1):65–70.

[2] Kania M, Rix H, Fereniec M, Zavala-Fernandez H, Janusek D, Mroczka T, Stix G, Maniewski R. The effect of precordial lead displacement on ecg morphology. Medical biological engineering computing 2014;52(2):109–119.

[3] Gillette K, Gsell MA, Prassl AJ, Karabelas E, Reiter U, Reiter G, Grandits T, Peyer C, Štern D, Urschler M, et al. A framework for the generation of digital twins of cardiac electrophysiology from clinical 12-leads ecgs. Medical Image Analysis 2021;102080.

[4] Gillette K, Gsell MA, Bouyssier J, Prassl AJ, Neic AV, Vigmond EJ, Plank G. Automated framework for the inclusion of a his-purkinje system in cardiac digital twins of ventricular electrophysiology. Annals of Biomedical Engineering 2021;.

[5] Wiedmann RT, Tan RC, Joyner RW. Discontinuous conduction at purkinje-ventricular muscle junction. American Journal of Physiology Heart and Circulatory Physiology 1996;271(4):H1507–H1516.

[6] Taggart P, Sutton PM, Opthof T, Coronel R, Trimlett R, Pugsley W, Kallis P. Inhomogeneous transmural conduction during early ischaemia in patients with coronary artery disease. Journal of molecular and cellular cardiology 2000; 32(4):621–630.

[7] Roberts DE, Scher AM. Effect of tissue anisotropy on extracellular potential fields in canine myocardium in situ. Circulation Research 1982;50(3):342–351.

[8] Bayer J, Blake R, Plank G, Trayanova N. A novel rule-based algorithm for assigning myocardial fiber orientation to computational heart models. Annuals of Biomedical Engineering 2012;40(10):2243–2254.

[9] Keller DU, Weber FM, Seemann G, Dossel O. Ranking the influence of tissue conductivities on forward-calculated ecgs. IEEE Transactions on Biomedical Engineering 2010; 57(7):1568–1576.

[10] Mitchell CC, Schaeffer DG. A two-current model for the dynamics of cardiac membrane. Bulletin of mathematical biology 2003;65(5):767–793.

[11] Neic A, Campos FO, Prassl AJ, Niederer SA, Bishop MJ, Vigmond EJ, Plank G. Efficient computation of electrograms and ecgs in human whole heart simulations using a reaction-eikonal model. Journal of computational physics 2017;346:191–211.

[12] Neic A, Gsell MA, Karabelas E, Prassl AJ, Plank G. Automating image-based mesh generation and manipulation tasks in cardiac modeling workflows using meshtool. SoftwareX 2020;11:100454.

Address for correspondence:

Karli Gillette
Neue Stiftingtalstraße 6/D04, A-8010 Graz, Austria
karli.gillette@medunigraz.at